Atmos. Chem. Phys. Discuss., 13, 6707–6728, 2013
www.atmos-chem-phys-discuss.net/13/6707/2013/
doi:10.5194/acpd-13-6707-2013

Atmospheric Chemistry and Physics Discussions
Open Access

Radiative and dynamical contributions to past and future Arctic stratospheric temperature trends

P. Bohlinger[1], B.-M. Sinnhuber[1], R. Ruhnke[1], and O. Kirner[2]

[1]Karlsruhe Institute of Technology, Institute for Meteorology and Climate Research, Karlsruhe, Germany
[2]Karlsruhe Institute of Technology, Steinbuch Centre for Computing, Karlsruhe, Germany

Received: 20 December 2012 – Accepted: 6 March 2013 – Published: 13 March 2013

Correspondence to: B.-M. Sinnhuber (bjoern-martin.sinnhuber@kit.edu)

Published by Copernicus Publications on behalf of the European Geosciences Union.

Abstract

Arctic stratospheric ozone depletion is closely linked to the occurrence of low stratospheric temperatures. There are indications that cold winters in the Arctic stratosphere have been getting colder, raising the question if and to what extent a cooling of the Arctic stratosphere may continue into the future. We use meteorological re-analyses from ERA-Interim for the past 32 yr together with calculations of the chemistry-climate model EMAC and CCM models from the CCMVal project to infer radiative and dynamical contributions to long-term Arctic stratospheric temperature changes. For the past three decades ERA-Interim shows a warming trend in winter and cooling trend in spring and summer. Changes in winter and spring are caused by a corresponding change of planetary wave activity with increases in winter and decreases in spring. During winter the increase of planetary wave activity is counteracted by a radiatively induced cooling. Stratospheric radiatively induced cooling is detected throughout all seasons being highly significant in spring and summer. This means that for a given dynamical situation, in ERA-Interim the annual mean temperature of the Arctic lower stratosphere has been cooling by $-0.41 \pm 0.11\,\mathrm{K\,decade^{-1}}$ at 50 hPa over the past 32 yr. Calculations with state-of-the-art models from CCMVal and the EMAC model confirm the radiatively induced cooling for the past decades, but underestimate the amount of radiatively induced cooling deduced from ERA-Interim. EMAC predicts a continued annual radiatively induced cooling for the coming decades (2001–2049) of $-0.15 \pm 0.06\,\mathrm{K\,decade^{-1}}$ where the projected increase of CO_2 accounts for about 2/3 of the cooling effect. Expected decrease of stratospheric halogen loading and resulting ozone recovery in the future counteracts the cooling tendency due to increasing greenhouse gas concentrations and leads to a reduced future cooling trend compared to the past. CCMVal multi-model mean predicts a future annual mean radiatively induced cooling of $-0.10 \pm 0.02\,\mathrm{K\,decade^{-1}}$ which is also smaller in the future than in the past.

ACPD

13, 6707–6728, 2013

1 Introduction

Large losses of Arctic stratospheric ozone have been observed during cold winters over the past decades (WMO, 2011). There is some evidence that the cold Arctic stratospheric winters are getting colder (Rex et al., 2004, 2006) with important implications for Arctic ozone depletion. In fact, the largest losses of Arctic stratospheric ozone have been observed in the recent winter 2010/2011 (Manney et al., 2011; Sinnhuber et al., 2011), despite the fact that the stratospheric halogen loading is already declining. Sinnhuber et al. (2011) calculated that a temperature trend of $-0.8\,\mathrm{K\,decade^{-1}}$ could enhance Arctic stratospheric ozone depletion enough to offset the recovery due to the expected future halogen decrease. Although there are still uncertainties in the climate sensitivity of Arctic ozone depletion, the calculated temperature sensitivity agrees well with the empirical results of Rex et al. (2006). Moreover, the calculated value of $-0.8\,\mathrm{K\,decade^{-1}}$ is close to the observed quasi-global cooling of the lower stratosphere of $-0.5\,\mathrm{K\,decade^{-1}}$ between 30 to 70 hPa by Randel et al. (2009). However, the situation in the Arctic is more complicated due to the large influence of planetary scale waves on Arctic winter and spring temperatures (Newman et al., 2001) and corresponding large inter-annual variability. Measurements indicate a strengthening of the Brewer-Dobson-Circulation (BDC) from December to February and a weakening from March until May connected to the increase/decrease of planetary wave activity, which leads to a corresponding positive/negative temperature trend (Fu et al., 2010). Recently, Thompson et al. (2012) have emphasized the existing large uncertainties for past temperature trends from observations in the mid-stratosphere (25–50 km altitude). However, in the lower stratosphere (15–20 km) Thompson et al. (2012) show good agreement between various satellite and radiosonde data sets, although most climate and chemistry-climate models underestimate the degree of this cooling.

In this study we analyze past and possible future temperature trends in the Arctic lower stratosphere. In particular, we investigate whether for a given level of planetary wave activity a cooling of the Arctic lower stratosphere can be identified. We

ACPD
13, 6707–6728, 2013

focus on temperatures in the lower stratosphere at 50 hPa, as this is the region most critical for Arctic ozone depletion. Unless otherwise noted we consider averages over 60–90° N. We use re-analyses from the European Centre for Medium Range Weather Forecasts (ECMWF) ERA-Interim project for the past 32 yr to determine temperature trends (Sect. 2). After comparing state-of-the art model calculations from CCMVal2 with the past temperature trends from ERA-Interim, these models are used to predict the evolution for the coming decades (Sect. 3). CCMVal2 models are accompanied by additional calculations with the chemistry-climate model EMAC. Sensitivity simulations with EMAC using fixed mixing ratios of greenhouse gases (in particular CO_2, N_2O, CH_4) and ozone depleting substances (ODS) are used to attribute future temperature changes to the respective trace gases.

2 Past Arctic temperature changes

ECMWF ERA-Interim re-analyses (Dee et al., 2011) from 1980–2011 are used to determine temperature trends. ERA-Interim data have been obtained from the ECMWF data server at a horizontal resolution of 1.5° × 1.5°. Temperature trends in the Arctic lower stratosphere are calculated, using daily temperature fields. The eddy heat flux, indicating planetary wave activity, is derived from daily temperature and wind fields at 100 hPa over 45–75° N (Newman et al., 2001).

Figure 1a shows ERA-Interim Arctic temperature changes at 50 hPa for the period 1980 to 2011. Values are given with a 2σ error range, meaning a 95.4 % confidence level. Averaged over the year there is cooling tendency of $-0.25 \pm 0.21\,\mathrm{K\,decade^{-1}}$. Summer months (JJA) show a significant cooling of $-0.42 \pm 0.13\,\mathrm{K\,decade^{-1}}$. This value is close to the quasi-global temperature trend of $-0.5\,\mathrm{K\,decade^{-1}}$ derived by Randel et al. (2009) in the lower stratosphere. Especially during summer, the Arctic stratosphere is in a state of radiative equilibrium which makes stratospheric temperature trends comparable to the quasi-global mean trend. Furthermore, there exists a strong significant cooling of $-1.02 \pm 0.58\,\mathrm{K\,decade^{-1}}$ during spring (MAM). In contrast, winter

ACPD
13, 6707–6728, 2013

months (DFJ) show a mean warming trend of $0.62 \pm 1.06\,\mathrm{K\,decade^{-1}}$, which is, however, not significant. Seasonal temperature trends from ERA-Interim are consistent with trends from Randel et al. (2009) derived from radiosonde data and are given in Table 2.

The cooling in spring and warming in winter is consistent with a corresponding change in wave activity, expressed by the area-weighted average of the eddy heat flux at 100 hPa over 45°–75° N (Fig. 2), which is consistent with findings from Fu et al. (2010). These changes in eddy heat flux thus lead to a dynamical contribution to long term Arctic temperature trends in ERA-Interim re-analyses.

Correlation between temperature and eddy heat flux are high exeeding $r = 0.75$ for all relevant months (December to May). This is consistent with findings from Newman et al. (2001) and allows us to use a multivariate regression method to separate the effects on temperature changes due to dynamical and radiative processes. For the multivariate regression we assume a linear trend term and a term referring to planetary wave activity being the eddy heat flux at 100 hPa integrated over the previous 45 days. The 45-day timescale corresponds to a typical radiative damping time at 50 hPa (Newman and Rosenfield, 1997; Newman et al., 2001). The dynamical contribution to the temperature trend therefore corresponds to the trends in eddy heat flux with the highest effect in winter and spring (Fig. 1b). The linear trend term represents the residual radiative conribution.

The radiative contribution (Fig. 1c) shows cooling throughout the whole year with an annual mean cooling of $-0.41 \pm 0.11\,\mathrm{K\,decade^{-1}}$, close to the cooling during summer, which is the same for the radiative contribution since planetary wave activity is low at that time. During winter the radiative contribution is negative ($-0.52 \pm 0.53\,\mathrm{K\,decade^{-1}}$) in contrast to the temperature trend mentioned above, which again shows the strong influence of planetary wave activity on lower stratospheric temperature in the Arctic. In spring, radiatively induced cooling is stronger compared to the other seasons and highly significant ($-0.76 \pm 0.35\,\mathrm{K\,decade^{-1}}$).

Due to the fact that temperatures in March are crucial for ozone destruction, we also investigate extended winter mean (DJFM) trends. Extended winter means show

ACPD
13, 6707–6728, 2013

radiative mean cooling of $-0.52 \pm 0.49\,\mathrm{K\,decade}^{-1}$, which is just significant at the 2σ level. Thus, for a given level of wave activity, mean winter temperatures have been getting colder over the past three decades by $-0.52 \pm 0.49\,\mathrm{K\,decade}^{-1}$. Again, this is comparable to the quasi-global mean cooling of about $-0.5\,\mathrm{K\,decade}^{-1}$ at this level from ERA-Interim (Table 3) and radiosonde observations (Randel et al., 2009).

3 Results from chemistry-climate models

3.1 Model description

To investigate if and how the inferred past cooling is expected to continue into the future we analyse results from 18 chemistry-climate model (CCM) simulations, performed as part of the second Chemistry-Climate Model Validation Activity (CCMVal2) (SPARC CCMVal, 2010). CCMVal2 model simulations used in this study refer to two sets of forcings, REF-B2 and SCN-B2d. REF-B2 models use greenhouse gas concentrations from A1B scenario (IPCC, 2000). Sea surface temperatures (SST) and sea ice concentrations (SIC) are simulated through previous offline model calculations. SCN-B2d additionally include volcanic eruptions, solar variability and a prescribed Quasi-Biennial Oscillation (QBO) of equatorial winds. Further information about CCMVal forcings can be found in the SPARC CCMVal (2010) report. For this study we use CCMVal2 model simulations listed in Table 1. Only models that reported monthly mean 100 hPa eddy heat flux based on daily fields are included. For the multivariate regression we use a mean of the eddy heat flux at 100 hPa consisting of the current and previous month which provides results similar to calculations with a damping time of 45 days.

In addition to CCMVal2 model simulations we performed further calculations with the ECHAM/MESSy Atmospheric Chemistry Model (EMAC). We use the Modular Earth Submodel System (MESSy) (Jöckel et al., 2005, 2006) in Version 1.7 in combination with ECHAM5 (Roeckner et al., 2006) as base model.

ACPD
13, 6707–6728, 2013

EMAC simulations were performed with a T42 horizontal resolution (about 2.8°) and 39 vertical levels with the uppermost level at 0.01 hPa. EMAC configurations basically follow the REF-B2 forcings and are briefly described in the following. SSTs and SICs were taken from a previous coupled simulation of the ECHAM5 climate model with the ocean model MPI-OM from Max-Planck-Institute in Hamburg. The A1B scenario (IPCC, 2007) was applied in the EMAC simulation. Volcanic eruptions, solar variability and QBO were not included according to REF-B2 conditions.

In this study, we focus on two periods. The first period is from 1980 to 2011 and the second from 2001 to 2049. The first period was chosen to allow a direct comparison with ERA-Interim. For future trends a starting point around 2000 is reasonable since the stratospheric halogen loading reached its maximum around that point and has been decreasing ever since (Kohlhepp et al., 2012). In the future, referring to A1B scenario, halogens continue to decrease. Choosing this period (2001–2049) enables the maximum halogen effect to become visible.

3.2 Reproducing the past

Figure 3a–c shows results from CCMVal2 simulations for 1980–2011, that can be directly compared to Fig. 1. Each black dot represents a single CCMVal2 model simulation with the black line being the multi-model mean over all CCMVal2 simulations. We do not find any distinct differences in temperature trends between REF-B2 and SCN-B2d, justifying the inclusion of both sets into the calculation of the multi-model mean. Our EMAC simulations, however, were not included in the multi-model mean.

Most CCMVal2 models show a cooling tendency in spring and summer (Fig. 3a) which is consistent with temperature trends from ERA-Interim re-analyses (Fig. 1a). In winter and early spring, however, there is a wide spread of the models reflecting large internal variability in these months. The range of dispersion of CCMVal2 models is about as large as ERA-Interim error bars, indicating that the variability between the models is consistent with the inter-annual variability of ERA-Interim re-analyses.

ACPD
13, 6707–6728, 2013

The dynamical component (Fig. 3b) shows no clear overall tendency but a wide spread of the participating models due to the aforementioned large internal variability. No clear strengthening of the 45°–75° N 100 hPa eddy heat flux in the last three decades can be identified.

The radiative contribution to temperature trends indicate a cooling tendency ($-0.16 \pm 0.04\,\mathrm{K\,decade^{-1}}$) of the CCMVal2 multi-model mean averaged over the year (Fig. 3c), which is even stronger in summer ($-0.22 \pm 0.02\,\mathrm{K\,decade^{-1}}$). The error on the multi-model mean is not shown in the figure. However, most CCMVal2 models underestimate ERA-Interim temperature trends, which is qualitively consistent with findings from Thompson et al. (2012). The CCMVal2 multi-model mean shows about half of the radiatively induced cooling of ERA-Interim. The spread of the models is smaller compared to Fig. 3a which is due to the missing variable dynamical contribution.

Our EMAC simulation is not part of the multi-model mean but shows a general agreement with most of the CCMVal2 models (Fig. 3). The variability of the EMAC model, displayed by the error bars, is comparable to ERA-Interim and is consistent with the spread of CCMVal2 models. In contrast to ERA-Interim re-analyses the dynamical and radiative contribution in EMAC have the same sign (Fig. 3b, c) during winter for 1980–2011, both contribute to a cooling.

EMAC shows a significant radiatively induced annual mean cooling of $-0.26 \pm 0.11\,\mathrm{K\,decade^{-1}}$. In fact, there is a cooling trend in all seasons (Table 2), however, underestimating the cooling in ERA-Interim. The cooling is significant for all seasons but winter. The strongest cooling accurs in spring, which is consistent with ERA-Interim.

3.3 Predicted future Arctic temperature changes

Future (2001–2049) temperature changes from the CCMVal2 and EMAC simulations are shown in Fig. 4a–c (similar to Figs. 1 and 3). Note that Fig. 4b, c have a different scale. CCMVal2 models show no clear temperature change in the future in any season (Fig. 4a). However, in summer there is a slight cooling indicated by the multi-model

ACPD
13, 6707–6728, 2013

mean but in each month models show both cooling and warming. Figure 4b shows again a large spread of the CCMVal2 models, when calculating the effect of planetary wave activity on the lower stratospheric temperature in the Arctic (cp. Fig. 3b). The multi-model mean shows a slight positive dynamical contribution, but is not significant. Considering only the radiative contribution the CCMVal2 multi-model mean for the future shows an annual cooling tendency of $-0.10 \pm 0.02\,\mathrm{K\,decade^{-1}}$ which is about 40 % smaller than the CCMVal2 multi-model mean for the past (1980–2011).

Our EMAC simulation shows cooling in summer, autumn and winter (Table 2), whereas in spring, there is a slight warming tendency. Annually averaged, there exists a cooling tendency of $-0.10 \pm 0.11\,\mathrm{K\,decade^{-1}}$. The dynamical component has no clear trend but contributes to warming in January until March and to cooling in December. As expected, these months are most affected by planetary wave activity in EMAC.

Compared to the period from 1980 to 2011 the radiative component shows a smaller, but significant cooling tendency with an annual temperature trend of $-0.15 \pm 0.06\,\mathrm{K\,decade^{-1}}$. The mean radiatively induced cooling in winter months has become clearer and continues into the future with $-0.26 \pm 0.37\,\mathrm{K\,decade^{-1}}$. In summer, trends become smaller compared to the past and decrease to $-0.15 \pm 0.05\,\mathrm{K\,decade^{-1}}$, while temperature changes in spring are slightly positive (Table 2).

3.4 Sensitivity study

In total, six EMAC simulations were performed. In addition to the standard simulation (EMAC STD) described above, five sensitivity simulations were calculated. In four simulations, mixing ratios of ODS (EMAC ODS), CO_2 (EMAC CO2), N_2O (EMAC N2O) and CH_4 (EMAC CH4) are held constant respectively for the period 2000 to 2049. One simulation was driven with all three major greenhouse gases (CO_2, N_2O and CH_4) fixed at 2000 (EMAC GHG). The simulations with fixed trace gases are initialised with data from the standard simulation until the year 2000.

ACPD
13, 6707–6728, 2013

Table 3 summarizes the calculated global mean temperature trends from the sensitivity simulations. Arctic seasonal temperature trends for the six EMAC simulations are shown in Fig. 5a. In summer, fixing CO_2 mixing ratio has the largest impact on future temperature trend which is thereby reduced to being negligible. Removing the small dynamical contribution in summer by multivariate regression (Fig. 5c) we can confirm that expected future increase of CO_2 contributes most to a radiatively induced cooling in the Arctic stratosphere. With a fixed CO_2 mixing ratio the summer temperature trend is reduced to $-0.05 \pm 0.04\,\mathrm{K\,decade^{-1}}$ compared to $-0.15 \pm 0.05\,\mathrm{K\,decade^{-1}}$ in EMAC STD. For constant CH_4 mixing ratio since 2000, there is less cooling of $-0.09 \pm 0.06\,\mathrm{K\,decade^{-1}}$ than in EMAC STD, meaning that an expected increase of CH_4 favours future cooling as well. Constant ODS result in a temperature trend of $-0.19 \pm 0.07\,\mathrm{K\,decade^{-1}}$. The expected decrease of ODS in the future and a corresponding ozone recovery in EMAC STD counteracts the cooling tendency due to increasing GHGs, leading to a slight warming tendency when all GHGs are held constant ($0.04 \pm 0.04\,\mathrm{K\,decade^{-1}}$). For N_2O EMAC calculations can identify only a minor radiative effect in summer. In the other seasons internal variability (Fig. 5b) is still high and cause large error bars, preventing a clear attribution.

4 Conclusions

We investigated past and possible future Arctic stratospheric temperature trends using ERA-Interim reanalyses, CCM calculations from the CCMVal2 project and additional calculations with the EMAC model. We focus on 50 hPa and averages over 60–90° N.

Arctic temperature trends over 1980–2011 from ERA-Interim show a warming in winter and cooling in spring and summer. The warming in winter and the cooling in spring is caused by a corresponding change in eddy heat flux with increases in winter and reductions in early and mid-spring.

Using multivariate regression, we separated temperature changes into a dynamical and a radiative component. We find that for a given level of eddy heat flux, there is a signifcant annual mean radiatively induced cooling in ERA-Interim of $-0.41 \pm 0.11\,\mathrm{K\,decade^{-1}}$, similar to the global mean cooling at 50 hPa. Moreover, the radiative contribution shows Arctic cooling in all months.

CCM calculations from CCMVal2 and EMAC reproduce the past radiatively induced cooling tendency. EMAC underestimates annual radiatively induced cooling compared to ERA-Interim ($-0.26 \pm 0.11\,\mathrm{K\,decade^{-1}}$), while the CCMVal2 multi-model mean shows even less cooling ($-0.16 \pm 0.04\,\mathrm{K\,decade^{-1}}$).

Calculations over the period 2001–2049 show continued cooling, but less than for the past. EMAC and the CCMVal2 multi-model mean expect the future radiative annual cooling to be about 40 % less compared to the past ($-0.15 \pm 0.06\,\mathrm{K\,decade^{-1}}$ and $-0.10 \pm 0.02\,\mathrm{K\,decade^{-1}}$, respectively). In order to explain these possible future temperature changes, we have performed additional sensitivity runs with the EMAC model. The resulting trends indicate that most of the future cooling in the Arctic lower stratosphere is due to the assumed increase in CO_2 and CH_4, where CO_2 accounts for about 2/3 of the radiatively induced cooling in summer. We find that the expected reductions of ODS and corresponding ozone recovery leads to a reduced cooling in the future, compared to past decades. However, future Arctic temperature trends during winter and spring are still associated with substantial uncertainties due to large internal variability and the non-linear feedback between temperature and ozone changes.

Acknowledgements. Parts of this work were supported by the Deutsche Forschungsgemeinschaft (DFG) through the Research Unit SHARP. ERA-Interim reanalyses were provided through the ECMWF data server. We acknowledge the modeling groups for making their simulations available for this analysis, the Chemistry-Climate Model Validation (CCMVal) Activity for WCRP's (World Climate Research Programme) SPARC (Stratospheric Processes and their Role in Climate) project for organizing and coordinating the model data analysis activity, and the British Atmospheric Data Center (BADC) for collecting and archiving the CCMVal model output.

The service charges for this open access publication have been covered by a Research Centre of the Helmholtz Association.

References

Dee, D. P., Uppala, S. M., Simmons, A. J., Berrisford, P., Poli, P., Kobayashi, S., Andrae, U., Balmaseda, M. A., Balsamo, G., Bauer, P., Bechtold, P., Beljaars, A. C. M., van de Berg, L., Bidlot, J., Bormann, N., Delsol, C., Dragani, R., Fuentes, M., Geer, A. J., Haimberger, L., Healy, S. B., Hersbach, H., Hólm, E. V., Isaksen, L., Kållberg, P., Köhler, M., Matricardi, M., McNally, A. P., Monge-Sanz, B. M., Morcrette, J.-J., Park, B.-K., Peubey, C., de Rosnay, P., Tavolato, C., Thépaut, J.-N., and Vitart, F.: The ERA-Interim reanalysis: configuration and performance of the data assimilation system, Q. J. R. Meteor. Soc., 137, 553–597, 2011. 6710

Fu, Q., Solomon, S., and Lin, P.: On the seasonal dependence of tropical lower-stratospheric temperature trends, Atmos. Chem. Phys., 10, 2643–2653, doi:10.5194/acp-10-2643-2010, 2010. 6709, 6711

IPCC 2000, N. Nakicenovic and R. Swart (Eds.): Emission Scenarios, Cambridge University Press, UK, Cambridge, England, 570 pp., 2000. 6712

IPCC 2007, Solomon, S., Qin, D., Manning, M., Marquis, M., Averyt, K., Tignor, M. M. B. and Miller, H. L. (Eds.): Climate Change 2007: Physical Science Basis. Contribution of Working Group I to the Fourth Assessment Report of the Intergovernmental Panel on Climate Change, Cambridge University Press, Cambridge, England, 2007. 6713

Jöckel, P., Sander, R., Kerkweg, A., Tost, H., and Lelieveld, J.: Technical Note: The Modular Earth Submodel System (MESSy) – a new approach towards Earth System Modeling, Atmos. Chem. Phys., 5, 433–444, doi:10.5194/acp-5-433-2005, 2005. 6712

Jöckel, P., Tost, H., Pozzer, A., Brühl, C., Buchholz, J., Ganzeveld, L., Hoor, P., Kerkweg, A., Lawrence, M. G., Sander, R., Steil, B., Stiller, G., Tanarhte, M., Taraborrelli, D., van Aardenne, J., and Lelieveld, J.: The atmospheric chemistry general circulation model ECHAM5/MESSy1: consistent simulation of ozone from the surface to the mesosphere, Atmos. Chem. Phys., 6, 5067–5104, doi:10.5194/acp-6-5067-2006, 2006. 6712

Kohlhepp, R., Ruhnke, R., Chipperfield, M. P., De Mazière, M., Notholt, J., Barthlott, S., Batchelor, R. L., Blatherwick, R. D., Blumenstock, Th., Coffey, M. T., Demoulin, P., Fast, H., Feng, W., Goldman, A., Griffith, D. W. T., Hamann, K., Hannigan, J. W., Hase, F., Jones, N. B., Kagawa, A., Kaiser, I., Kasai, Y., Kirner, O., Kouker, W., Lindenmaier, R., Mahieu, E., Mittermeier, R. L., Monge-Sanz, B., Morino, I., Murata, I., Nakajima, H., Palm, M., Paton-Walsh, C., Raffalski, U., Reddmann, Th., Rettinger, M., Rinsland, C. P., Rozanov, E., Schneider, M., Senten, C., Servais, C., Sinnhuber, B.-M., Smale, D., Strong, K., Sussmann, R., Taylor, J. R., Vanhaelewyn, G., Warneke, T., Whaley, C., Wiehle, M., and Wood, S. W.: Observed and simulated time evolution of HCl, $ClONO_2$, and HF total column abundances, Atmos. Chem. Phys., 12, 3527–3556, doi:10.5194/acp-12-3527-2012, 2012. 6713

Manney, G. L., Santee, M. L., Rex, M., Livesey, N. J., Pitts, M. C., Veefkind, P., Nash, E. R., Wohltmann, I., Lehmann, R., Froidevaux, L. et al.: Unprecedented Arctic ozone loss in 2011, Nature, 478, 469–475, doi:10.1038/nature10556, 2011. 6709

Newman, P. A. and Rosenfield, J. E.: Stratospheric thermal damping times, Geophys. Res. Lett., 24, 433–436, 1997. 6711

Newman, P. A., Nash, E. R., and Rosenfield, J. E.: What controls the temperature of the Arctic stratosphere in March?, J. Geophys. Res., 106, 19999–20010, 2001. 6709, 6710, 6711

Randel, W. J., Shine, K. P., Austin, J., Barnett, J., Claud, C., Gillett, N. P., Keckhut, P., Langematz, U., Lin, R., Long, C., Mears, C., Miller, A., Nash, J., Seidel, D. J., Thompson, D. W. J., Wu, F. and Yoden, S.: An update of observed stratospheric temperature trends, J. Geophys. Res., 114, D02107, doi:10.1029/2008JD010421, 2009. 6709, 6710, 6711, 6712, 6722

Rex, M., Salawitch, R. J., von der Gathen, P., Harris, N. R. P., Chipperfield, M. P., and Naujokat, B.: Arctic ozone loss and climate change, Geophys. Res. Lett., 31, L04116, doi:10.1029/2003GL018844, 2004. 6709

Rex, M., Salawitch, R. J., Deckelmann, H., von der Gathen, P., Harris, N. R. P., Chipperfield, M. P., Naujokat, B., Reimer, E., Allaart, M., Andersen, S. B., Bevilacqua, R., Braathen, G. O., Claude, H., Davies, J., De Backer, H., Dier, H., Dorokhov, V., Fast, H., Gerding, M., Godin-Beekmann, S., Hoppel, K., Johnson, B., Kyrö, E., Litynska, Z., Moore, D., Nakane, H., Parrondo, M. C., Risley Jr., A. D., Skrivankova, P., Stübi, R., Viatte, P., Yushkov, V., and Zerefos, C.: Arctic winter 2005: implications for stratospheric ozone loss and climate change, Geophys. Res. Lett., 33, L23808, doi:10.1029/2006GL026731, 2006. 6709

Roeckner, E., Brokopf, R., Esch, M., Giorgetta, M. Hagemann, S., and Kornblueh, L.: Sensitivity of simulated climate to horizontal and vertical resolution in the ECHAM5 atmosphere model, J. Climate, 19, 3771–3791, 2006. 6712

Sinnhuber, B.-M., Stiller, G., Ruhnke, R., von Clarmann, T., Kellmann, S., and Aschmann, J.: Arctic winter 2010/2011 at the brink of an ozone hole, Geophys. Res. Lett., 38, L24814, doi:10.1029/2011GL049784, 2011. 6709

ACPD
13, 6707–6728, 2013

SPARC CCMVal, Eyring, V., Shepherd, T. G., and Waugh, D. W. (Eds.): SPARC Report on the Evaluation of Chemistry-Climate Models, SPARC Report No. 5, WCRP-132, WMO/TD-No. 1526, available at: http://www.atmosp.physics.utoronto.ca/SPARC (last access: December 2012), 2010. 6712

Thompson, D. W. J., Seidel, D. J., Randel, W. J., Zou, C.-Z., Butler, A. H., Mears, C., Osso, A., Long, C. and Lin, R.: The mystery of recent stratospheric temperature trends, Nature, 491, 692–697, doi:10.1038/nature11579, 2012. 6709, 6714

WMO: Scientific Assessment of Ozone Depletion: 2010, Global Ozone Research and Monitoring Project – Report No. 52, World Meteorological Organization, Geneva, Switzerland, 516 pp., 2011. 6709

ACPD
13, 6707–6728, 2013

Arctic stratospheric temperature trends

P. Bohlinger et al.

Table 1. Model calculations used in this study. Only CCMVal2 models that reported 100 hPa eddy heat flux are included. Numbers in parenthesis indicate number of ensemble members included.

CCMVal2 REF-B2 model runs
CCSRNIES (1)
CMAM (3)
GEOSCCM (1)
LMDZepro (1)
MRI (2)
Niwa SOCOL (1)
SOCOL (3)
ULAQ (3)
UMUKCA-METO (1)
CCMVal2 SCN-B2d model runs
E39CA (1)
EMAC-FUB (1)
Additional EMAC runs
EMAC REF-B2 standard run (1)
EMAC GHGs constant after 2000 (1)
EMAC CO_2 constant after 2000 (1)
EMAC CH_4 constant after 2000 (1)
EMAC N_2O constant after 2000 (1)
EMAC ODSs constant after 2000 (1)

ACPD
13, 6707–6728, 2013

Table 2. Arctic temperature trends (60–90° N) at 50 hPa from ERA-Interim reanalyses and model simulations. Seasonal temperature trends (overall) are shown for ERA-Interim. The radiative contribution to the temperature trend is shown for ERA-Interim, CCMVal2 multi-model mean and our EMAC simulation. Values from Randel et al. (2009) are given for 1979–2007, with uncertainty estimates given only for DFJ and JJA. All values are in K/decade with a 2σ error range.

Data set	DJF	MAM	JJA	SON	Annual
1980–2011					
ERA-Interim (overall)	+0.63 ± 1.06	−1.02 ± 0.58	−0.42 ± 0.13	−0.12 ± 0.22	−0.25 ± 0.21
ERA-Interim (radiative)	−0.52 ± 0.53	−0.76 ± 0.35	−0.42 ± 0.13	−0.11 ± 0.16	−0.41 ± 0.11
EMAC (radiative)	−0.26 ± 0.52	−0.44 ± 0.36	−0.24 ± 0.10	−0.25 ± 0.19	−0.26 ± 0.11
CCMVal2 (radiative)	−0.03 ± 0.08	−0.30 ± 0.11	−0.22 ± 0.02	−0.14 ± 0.05	−0.16 ± 0.04
Randel et al. (2009)	−0.32 ± 0.52	−0.76	−0.59 ± 0.32	−0.16	
2001–2049					
EMAC (radiative)	−0.26 ± 0.37	+0.11 ± 0.21	−0.15 ± 0.05	−0.31 ± 0.10	−0.15 ± 0.06
CCMVal2 (radiative)	−0.17 ± 0.04	−0.03 ± 0.06	−0.08 ± 0.01	−0.13 ± 0.02	−0.10 ± 0.02

Discussion Paper | Discussion Paper | Discussion Paper | Discussion Paper |

ACPD

13, 6707–6728, 2013

Arctic stratospheric temperature trends

P. Bohlinger et al.

Table 3. Global temperature trends at 50 hPa from ERA-Interim reanalyses and model simulations. All values are in $K\,decade^{-1}$ with a 2σ error range.

Data set	Annual mean trend
1980–2011	
ERA-Interim	-0.46 ± 0.05
EMAC	-0.20 ± 0.03
CCMVal2	-0.314 ± 0.004
2001–2049	
EMAC (STD)	-0.30 ± 0.02
CCMVal2	-0.224 ± 0.002
EMAC const. ODS	-0.32 ± 0.02
EMAC const CO_2	-0.10 ± 0.03
EMAC const. N_2O	-0.28 ± 0.02
EMAC const. CH_4	-0.24 ± 0.03
EMAC const. GHGs	-0.06 ± 0.02

ACPD
13, 6707–6728, 2013

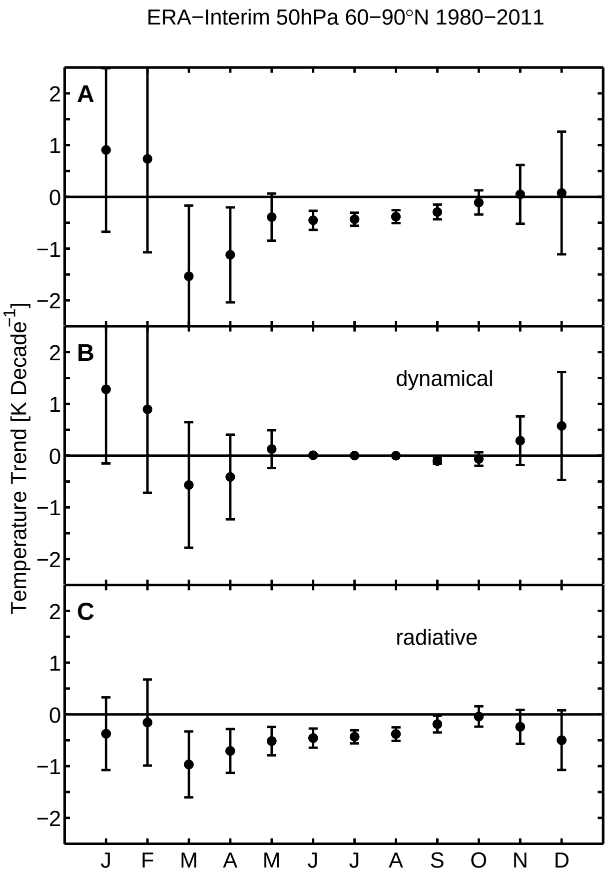

Fig. 1. Arctic temperature trends per decade at 50 hPa for each month from ERA-Interim for the years 1980–2011. The figure shows the area-weighted average over 60–90° N. **(A)** Temperature trend. **(B)** Dynamical component of the trend. **(C)** Radiative component of the trend. Vertical bars show the 2σ uncertainty.

ACPD
13, 6707–6728, 2013

Arctic stratospheric temperature trends

P. Bohlinger et al.

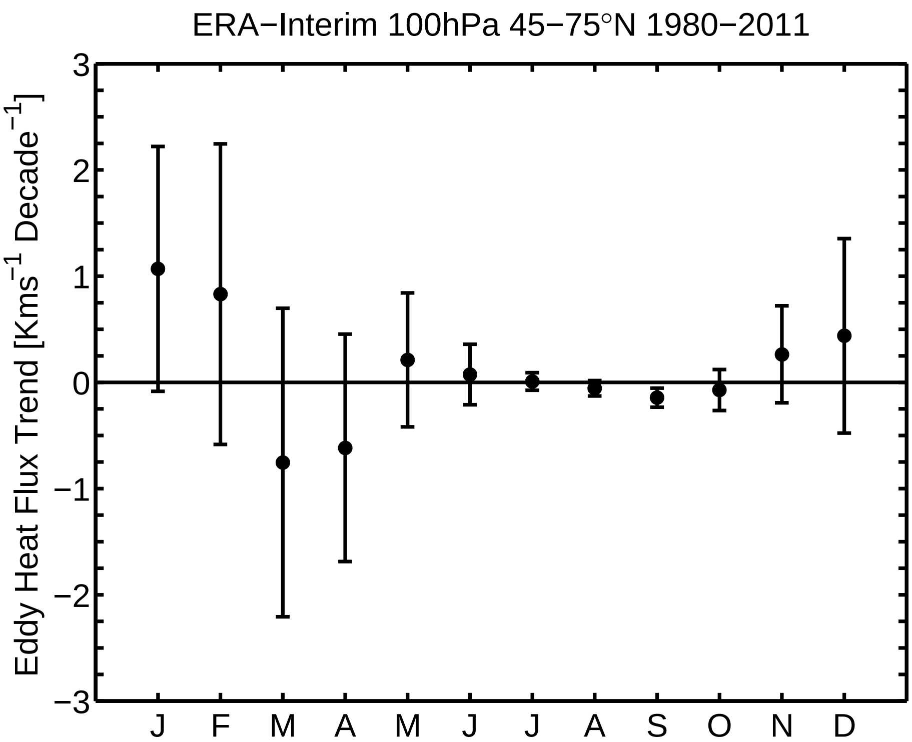

Fig. 2. Eddy heat flux trend at 100 hPa from ERA-Interim data (1980–2011). The figure shows the area-weighted average over 45–75° N. Mean trends are calculated of eddy heat flux averages over the previous 45 days. Vertical bars show the 2σ uncertainty.

ACPD
13, 6707–6728, 2013

Arctic stratospheric temperature trends

P. Bohlinger et al.

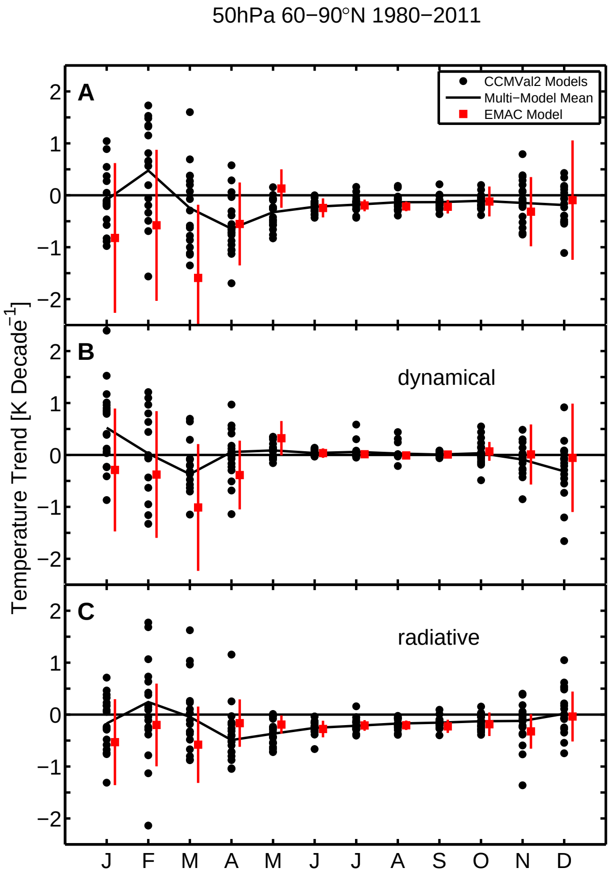

Fig. 3. Arctic temperature trends per decade at 50 hPa for each month from EMAC (red) and CCMVal2 models (black) for the years 1980–2011. The figure shows the area-weighted average over 60–90° N. **(A)** Temperature trend. **(B)** Dynamical component of the trend. **(C)** Radiative component of the trend. Vertical bars show the 2σ uncertainty.

ACPD
13, 6707–6728, 2013

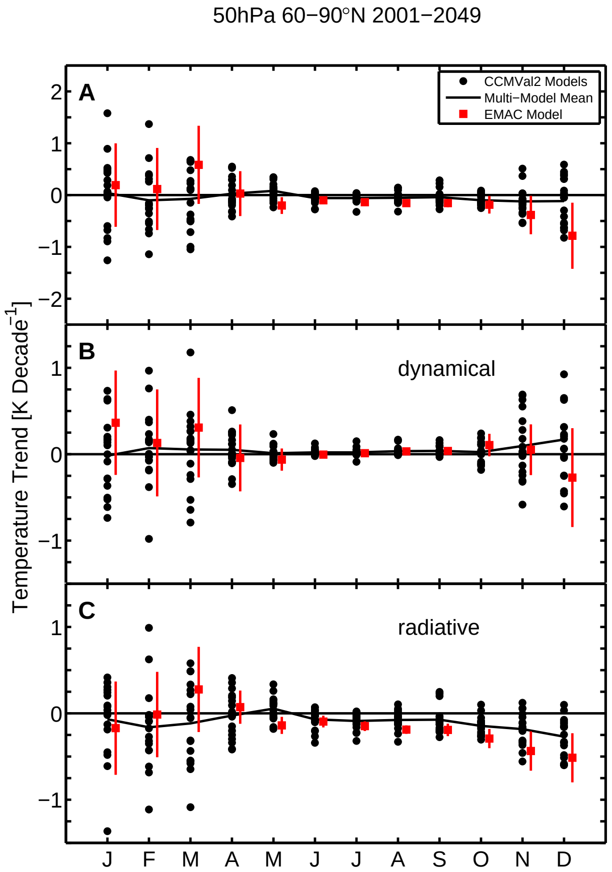

Fig. 4. Arctic temperature trends per decade at 50 hPa for each month from EMAC (red), EMAC CO2 (blue), EMAC ODS (orange) and CCMVal2 models (black) for the years 2001–2049. The figure shows the area-weighted average over 60–90° N. **(A)** Temperature trend. **(B)** Dynamical component of the trend. **(C)** Radiative component of the trend. Vertical bars show the 2σ uncertainty. Note the different scale for **(B)** and **(C)**.

ACPD
13, 6707–6728, 2013

Title Page
Abstract Introduction
Conclusions References
Tables Figures
◂ ▸
Back Close
Full Screen / Esc
Printer-friendly Version
Interactive Discussion

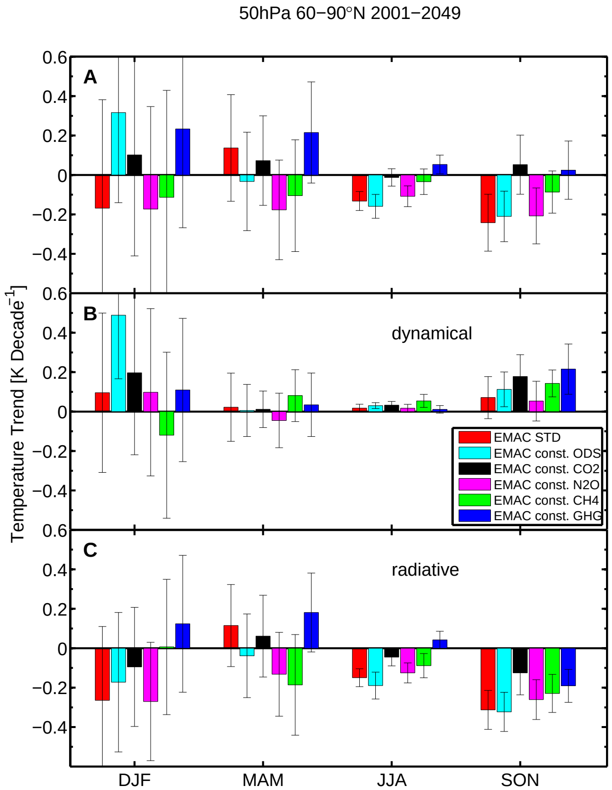

Fig. 5. Arctic temperature trends per decade at 50 hPa for each month from EMAC STD (red), EMAC ODS (cyan), EMAC CO2 (black), EMAC N2O (magenta), EMAC CH4 (green) and EMAC GHG (blue) for the years 2001–2049. The figure shows the area-weighted average over 60–90° N. **(A)** Temperature trend. **(B)** Dynamical component of the trend. **(C)** Radiative component of the trend. Vertical bars showing the 2σ uncertainty for all model simulations.